ARCHITECTURAL RESEARCH, Vol. 2, No.1(2000), pp.61-69

Hysteretic Energy Characteristics of Steel Moment Frames Under Strength Variations

Byong Jeong Choi
Department of Architecture, Seoul National University, Seoul, Korea

Duck Jae Kim
Department of Architectural Engineering, Chung-Ang University, Seoul, Korea

Abstract

This research focused on the hysteretic energy performance of 12 steel moment-resisting frames, which were intentionally designed by three types of design philosophies, strength control design, strength and drift control design, and strong-column and weak-beam control design. The energy performances of three designs were discussed in view of strength increase effect, stiffness increase effect, and strong-column and weak-beam effects. The mean hysteretic energy of the 12 basic systems were statically processed and compared to that of single-degree-of-freedom systems. Hysteretic energy was not always increased with an increase of strength and stiffness in the steel moment-resisting frames. Hysteretic energy between strong-column and weak-beam design and drift control design with the same stiffness was not sensitive each other for these types of mid-rises of steel moment-resisting frames.

Keywords: Steel structure, strong-column and weak-beam, hysteretic energy input, earthquake

1. INTRODUCTION

For many years earthquake engineers have tried to find out better parameters to express the potential damage of buildings (Housner, 1956; Berg & Thomaides, 1960; Arias, 1969; Fajfar & Fischinger, 1990; Uang & Bertero, 1990; Schneider et al., 1993). One of the ways to prevent the potential damages of buildings due to earthquakes is to understand the hysteretic energy (E_h) of a structural system (Iwan & Gates, 1979). In this research, the E_h of different structural systems was discussed. The seismic design philosophy for usual building structures relies strongly on E_h. The energy to a structure subjected to ground motions is dissipated in part by inelastic deformation (E_h) and partially by viscous damping energy which represents miscellaneous damping effects other than E_h.

The energy can be expressed as:

$$m\ddot{u} + c\dot{u} + f_S(u,\dot{u}) = -m\ddot{u}_g(t)$$

$$\int_0^u m\ddot{u}(t)du + \int_o^u c\dot{u}(t)du + \int_0^u f_s(u,\dot{u})du = -\int_0^u m\ddot{u}_g(t)du$$

For any structure, total energy (E_{out}) must be equal to total internal energy (E_{int}) supplied. It can be represented as $E_{out} = E_{int}$. Internal energy consists of kinetic energy (E_k), strain energy (E_s), damping energy (E_D), and E_h.

Housner (1956) expressed the above relationship as $E_{out} = E_k + E_s + E_D + E_h$.

Hitherto, a few investigations have been carried out on the E_h of structure. Zarah and Hall (1982) and Akiyama (1985) have found out the proportion of energy dissipated by yielding increases with an decrease of viscous damping and the decrease of the displacement ductility of a structural system. Based on their observations it is apparent that the E_h is a function of damping and strength rather than ductility. However, Kuwamura and Galambos (1989) insisted that the E_h was depended on viscous damping and accumulative ductility. It has been known that the strength of structural systems affects the E_h (Choi, 1998, 2000).

Vidic et al. (1991) proposed to draw a strength effect using single-degree-of-freedom (SDOF) systems. They explored the E_h using parameters such as initial stiffness (period), strength, and hysteretic behavior and ground motions. In their research, the ratio, hysteretic energy/total energy, was used to evaluate the influence of strength. They found out the increase of strength decreases the E_h. The stiffness-proportional damping and SDOF systems were used to draw the strength effects. Based on these investigations, both the strength effects and damping effects are crucial to the E_h and both mass-proportional and stiffness-proportional dampings are important to understand the E_h. However, in our study, Rayleigh damping was used to simplify the structure. The elasto-plastic model was used in the analysis. Many of current observations focused on SDOF systems. However, it is not clear whether the interpretation of E_h between SDOF systems and mult-degree-of-freedom (MDOF) systems is similar or not (Leger & Dussault, 1992). Therefore authors tried to observe the influence of strength using MDOF systems. For the strength study based on E_h, the 12 steel MDOF systems were designed to compare different strength effects. The basic structure of this study was technically modified to explore strength effect of MDOF systems. Based on 12 steel moment frames using five earthquake ground motions, the empirical E_h

Table 1. Characteristics of Earthquake Ground Motions

No.	Ground Motion	Component	Distance Km	A/g	u_{g0} cm/s	t_g s	t_D s	Geology
EQ 1	El Centro May 18, 1940	S00E	10.8	0.3489	33.45	0.55	24.46	Stiff Soil
EQ 2	Taft 1952	N21E	12.2	0.1556	15.69	0.70	28.84	Rock
EQ 3	Parkfield June 27, 1966	N65E	9.8	0.4891	78.08	0.68	6.44	Stiff Soil
EQ 4	Olympia April 13, 1949	N04W	11.4	0.1647	21.41	1.20	21.64	-
EQ 5	Northridge Jan. 17, 1994	New-360	10.2	0.5963	56.9	0.68	5.50	Alluvium

function was provided.

2. MODELING

2.1 Design of Earthquake Level

To examine the characteristics of selected earthquake ground motions, response spectrum analysis was performed using the SPECEQ program (Nigam & Jennings, 1968). Even though damping effect is important for the observation of E_h, the Rayleigh damping of 2% was adopted in this study. Generally, higher modes are effective on E_h in nonlinear analysis.

In our study, the first and third modes were used because preliminary mode analysis showed that the higher E_h resulted from that mode combination. Two design earthquake levels (DEQL) of 0.3g (DEQL I) and 0.6g (DEQL II) were used. To perform the proposed energy sensitivity studies, nonlinear time history analysis was used for the MDOF systems.

A total of five ground motions was used and scaled to the targeted peak ground accelerations (PGA) which were the DEQL I and DEQL II. Five ground motions were carefully selected by considering alluvium soil conditions from western areas. The detailed characteristics of ground motions are shown in Table 1. The plots of the time history and the normalized response of earthquake ground motions are shown in Fig. 1 and 2. The notations for modeling are shown in Table 2.

2.2 Loading Assumptions of MDOF System

To perform nonlinear dynamic analysis, the DRAIN-2DX program (Powell et al., 1993) was used in this study. The plastic hinges were assumed to occur at the ends of an element. No rigid zone was considered and the beam-column element (type 02) was used in the program. The nominal yield strengths of beam and column were assumed by 24.82 and 34.47 kN/cm^2, respectively. Dead load and live load for roof were 0.2873 N/cm^2 and 0.1436 N/cm^2, and those for floor were 0.4309 N/cm^2 and 0.3352 N/cm^2, respectively. The relative energy was used to define the work done by equivalent force (mass multiplied by the ground acceleration) on the equivalent fixed based system. The rigid body translation on the structure was not considered in this study. The straining hardening by 2% was used for the MDOF systems. The Raleigh damping considering the first and the third modes was used for MDOF systems.

2.3 Design of Basic Systems with Three Design Philosophies

The steel moment perimeter frames in two- and six-story were designed with different design concepts. The overall schedules of modeling for MDOF systems is shown in Table 3. Three design philosophies called the basic systems were strength control (S), strength and drift control (SD), and strong-column and weak-beam control (SDS).

Table 2. Descriptions of Modeling (SDS).

Name	Notation	Name	Notation
El Centro	EQ 1	2-story-SCWB-3 span	2SDS3
Taft	EQ 2	2-story –strength-6 span	2S6
Parkfield	EQ 3	2-story-drift-6 span	2SD6
Olympia	EQ 4	2-story-SCWB-6 span	2SDS6
New Hall	EQ 5	6-story –strength-3 span	6S3
Strength design	S	6-story-drift-3 span	6SD3
Drift design	SD	6-story-SCWB-3 span	6SDS3
SCWB design	SDS	6-story –strength-6 span	6S6
Modified SD	MSD	6-story-drift-6 span	6SD6
2-story 3-span	2-3SP	6-story-SCWB-6 span	6SDS6
2-story 6-span	2-6SP	Design Earthquake Level 1	DEQL I
6-story 3-span	6-3SP	Design Earthquake Level 2	DEQL II
6-story 6-span	6-6SP		

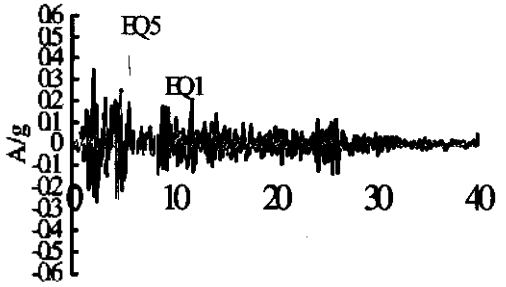

Fig. 1 Time histories of El Centro (EQ 1) and Northridge (EQ 5) earthquake

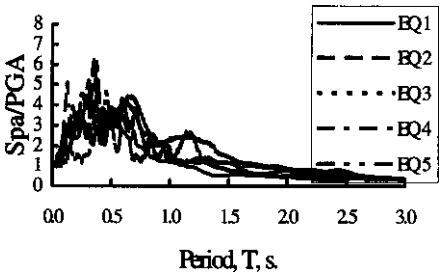

Fig. 2 Response spectrum of earthquake ground motion

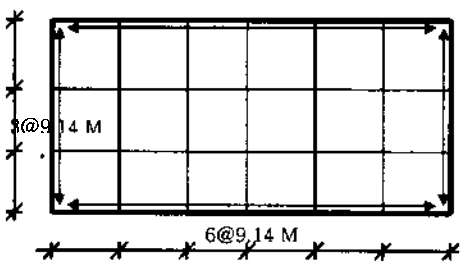

Fig. 3 Plan view of SMRF in perimeter

The load resistant factor design (LRFD) method and the equivalent lateral force method by uniform building code-1997(UBC-97) were used to design the basic systems. The plan view of the MDOF system is shown in Fig. 3. The beam and column schedules in 3-span (3-SP) and 6-span (6-SP) of steel moment perimeter frames are shown in Table 4, 5, 6, and 7. The UBC-97 was used to determine the design base shear (V) of the frames. In the design of the steel moment resisting frames, the 3-SP of the plan view was designed first. Next, the direction of 6-SP in plan view was designed. The exterior columns from the design of the 3-SP were not changed in the authors' design of the 6-SP. The design S means that the strength controls the design where both the drift limitation of UBC-97 Code and SDS condition was not observed. It was designed only to consider the strength at given condition. Therefore, the plastic hinges occurred at any place of beams and columns (Fig. 4a and 5a).

Table 3. Schedule of Basic Systems

No.	Target System	T	V/W	Observed plastic hinge from pushover analysis
1	2S3	0.94	0.25	Beam and column
2	2SD3	0.82	0.27	Column
3	2SDS3	0.68	0.45	Beam and column
4	2S6	0.92	0.26	Beam and column
5	2SD6	0.82	0.26	Column
6	2SDS6	0.74	0.39	Beam and column
7	6S3	2.01	0.13	Beam and column
8	6SD3	1.48	0.15	Column
9	6SDS3	1.41	0.23	Beam and column
10	6S6	1.87	0.14	Beam and column
11	6SD6	1.38	0.15	Column
12	6SDS6	1.41	0.22	Beam and column

Table 4. Beam and Column Schedule for 3 Spans of 2-Story

Story	S		SD		SDS	
	Beam	Column	Beam	Column	Beam	Column
2	W460x74	W360 x179 * (W360x91)	W610x 113	W360x179 (W360x91)	W610x 113	W360x26 2 (W360x16 2)
1	W610x11 3	W360x179 (W360x91)	W760x 173	W360x179 (W360x91)	W760x 173	W360x26 2 (W360x16 2)

* ( ) is exterior column.

Table 5. Beam and Column Schedule for 6 Spans of 2-Story

Story	S		SD		SDS	
	Beam	Column	Beam	Column	Beam	Column
2	W460x 74	W610x 82 (W360x91)	W460x 74	W360x101 (W360x91)	W460x 74	W360x 162 (W360x16 2)
1	W610x 82	W360x101 (W360x91)	W760x 147	W360x101 (W360x91)	W610x 82	W360x 162 (W360x16 2)

The design of SD frame means that both the strength and drift limitations are considered for frame SD. In the design of the frame SD, the beam sections for each floor was arbitrarily increased after the design of frame S. Therefore, the plastic hinges occurred in the columns (Fig. 4b and 5b). In this design, the drift limitation due to lateral forces was observed. The drift limitation δ / h for current UBC-97 was by 3.36% for these design cases. In the design of frame SDS, the strong column-weak beam regulation by LRFD was observed. The drift limitation of UBC-97 was also kept. The plastic hinges occurred at the ends of beams. The plastic hinges of columns were smaller than those of beams (Fig. 4c and 5c). The similar patterns

of plastic hinges were acquired from the 6-story frames. The plastic hinge patterns of 6-story frames were omitted. The MDOF systems were subjected to the five earthquake ground motions at two levels of intensities by DEQL I (0.3g) and DEQL II (0.6g). In the study the peak ground accelerations of each ground motion were vary. Thus, the authors scaled earthquakes to two levels of intensities to investigate the energy input at an target intensity.

Table 6. Beam and Column Schedule for 3 Spans of 6-Story

Story	S		SD		SDS	
	Beam	Column	Beam	Column	Beam	Column
6	W460x74	W360x122 (W360x79)	W760x147	W360x122 (W360x79)	W610x82	W360x262 (W360x162)
5	W610x113	W360x122 (W360x79)	W1000x693	W360x122 (W360x79)	W840x173	W360x262 (W360x162)
4	W690x125	W360x179 (W360x162)	W1000x883	W360x179 (W360x162)	W840x176	W360x382 (W360x216)
3	W760x134	W360x179 (W360x162)	W1000x883	W360x179 (W360x162)	W920x238	W360x382 (W360x216)
2	W760x147	W360x262 (W360x216)	W1000x883	W360x262 (W360x216)	W920x238	W360x421 (W360x287)
1	W760x173	W360x262 (W360x216)	W1000x883	W360x262 (W360x216)	W920x238	W360x421 (W360x287)

Table 7. Beam and Column Schedule for 6 Spans of 6-Story

Story	S		SD		SDS	
	Beam	Column	Beam	Column	Beam	Column
6	W460x60	W360x101 (W360x79)*	W460x60	W360x101 (W360x791)	W460x74	W360x162 (W360x162)
5	W610x82	W360x101 (W360x101)	W920x289	W360x101 (W360x791)	W610x125	W360x162 (W360x162)
4	W610x101	W360x162 (W360x162)	W920x289	W360x162 (W360x162)	W890x125	W360x262 (W360x216)
3	W610x101	W360x162 (W360x162)	W920x289	W360x162 (W360x162)	W760x147	W360x262 (W360x216)
2	W610x113	W360x179 (W360x216)	W920x289	W360x179 (W360x216)	W760x161	W360x262 (W360x287)
1	W610x140	W360x179 (W360x216)	W1000x745	W360x216 (W360x216)	W760x161	W360x262 (W360x287)

* ( ) is exterior column, AISC

2.4 Design of Modified System (MSD)

Pushover technique was used to match frame SD to frame SDS based on the base shear coefficient (V/W) and the natural period of a system. The masses of the SD frames for the 2-story (2SD3 and 2SD6) and 6-story (6SD3 and 6SD6) in both directions were decreased or increased to match the period to that of SDS frame.

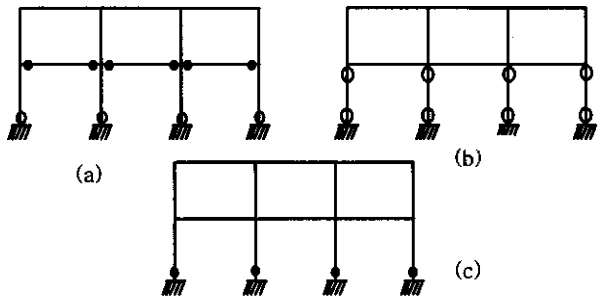

Fig.4 Plastic mechanisms of 2S3, 2SD3, and 2SDS3 designs by pushover at u = 1.2

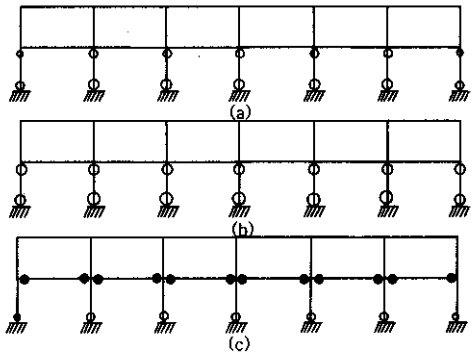

Fig.5 Plastic mechanisms of 2S6, 2SD6, and 2SDS6 by pushoverat u=1.2.

The M_p was increased gradually until the strength and slope reached the same V/W of the frame SDS. Then, the modified basic system (MSD) was constructed by the modification above.

Due to the modification, the masses of 6MSD3 and 6MSD6 were 17.5635 (kN/cm/sec^2) and 19.8504 (kN/cm/sec^2), respectively. The masses of 2MSD3 and 2MSD6 were 4.0291 kN/cm/sec^2 and 4.7576 kN/cm/sec^2, respectively. Note that the original masses of the 2-story and the 6-story were 5.8672 kN/cm/sec^2 and 19.0879 kN/cm/sec^2, respectively. Therefore, the masses were controlled to match the period of SD to the one of SDS, and the M_p was changed to match the frame SDS. After the set-up of the MSD, the frame MSD was compared with the basic systems of 2SDS3, 2SDS6, 6SDS3, and 6SDS6. The static pushover method was introduced to acquire the same maximum base shear coefficient (V/W) and period (T) through the modification. Therefore, the basic structural characteristics of the two systems (MSD and SDS) were the same V/W. Thus, the design concepts were different from each other; the MSD frames were WCSB systems and the SDS frames were SCWB systems.

The steps are summarized as follows:

(1) Reduce or increase the weights at each floor by the same ratio. If T_i reaches the target period, stop the reducing or increasing the weight (W).

(2) Increase the nominal yield strength F_y of beams and

columns proportionally until the yield shear force reaches the target yield shear force of frame SDS.

(3) Finally, pushover analysis is carried out to see the ratio V/W to roof deformation. After the modifications, the pushover results of all basic systems are shown in Fig. 6.

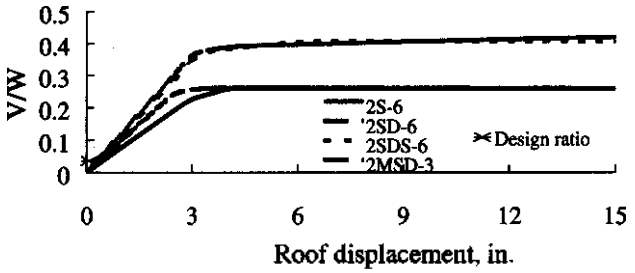

Fig. 6 Pushover analysis results of basic systems

3. RESULTS AND DISCUSSION

3.1 Effects of Stiffness and Strength Increase (S versus SDS)

From the pushover analysis, the frame SDS had higher strength and stiffness compared to the frame S (Fig. 6). It is believed that the E_h decreased with an increase of strength in a SDOF system for short and longer periods. However, for the medium periods between 0.5 sec and 1.0 sec., the E_h was increased with an increase of design strength coefficients (Fig. 7).

At DEQL I, the E_h decreased with an increase of base shear coefficient (V/W) for the 2-6SP, 6-3SP, 6-6SP under EQ 1 (Fig. 8). This behavior well supported the general recognition that the E_h to a system having high strength was smaller than that of a system having lower strength (V/W). This result is explained in Fig. 9 where the E_h of frame SDS are clearly smaller than that of S for all frames at EQ 5, the level of DEQL I.

However, somewhat different results came out when the intensity of ground motion increased from DEQL I to DEQL II. The E_h increased with the increase of strength and stiffness for the frames of 2-3SP and 2-6SP at EQ 1, DEQL II (Fig. 10). In other word, the E_h of frame SDS is greater than that of frame S at EQ 1, DEQL II. In the case of EQ 5 at DEQL II, the E_h of frame SDS was greater than that of frame S for every frame. The E_h of frame SDS increased about from 22% to 52% for EQ 5, DEQL II (Fig. 11). These increases resulted from the increase of the ground motion intensity and the increase of the periods of frames. The increase of E_h for 2-story frames was also contributed from the change of periods ranging from 0.68 sec to 0.94 sec in the first mode. It was also found out that the E_h of these ranges increased with an increase of V/W for SDOF systems (Choi, 1998)

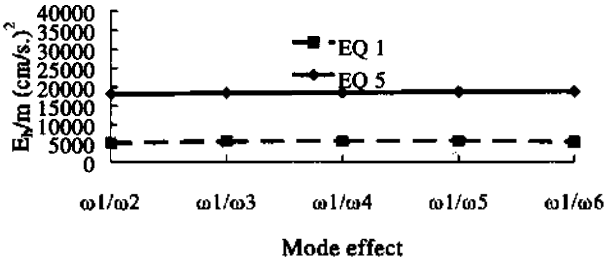

Fig. 7 Mode effects on E_h, 6SDS, DEQL II

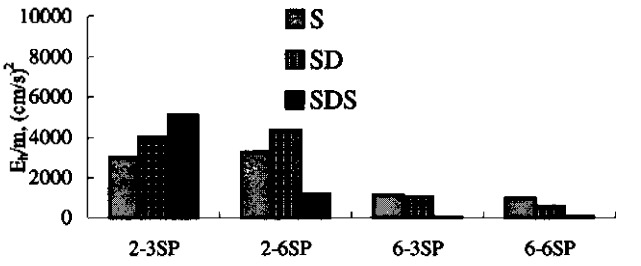

Fig. 8 Eh/m with EQ 1, DEQL I

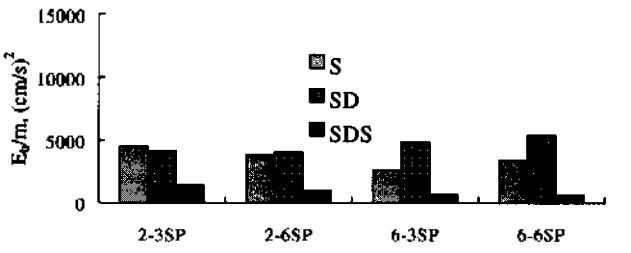

Fig. 9 Eh/m with EQ 5, DEQL I

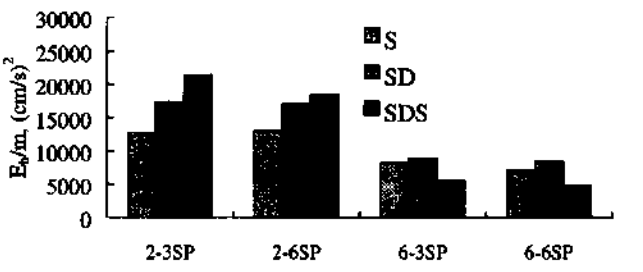

Fig. 10 Eh/m with EQ 1, DEQL II

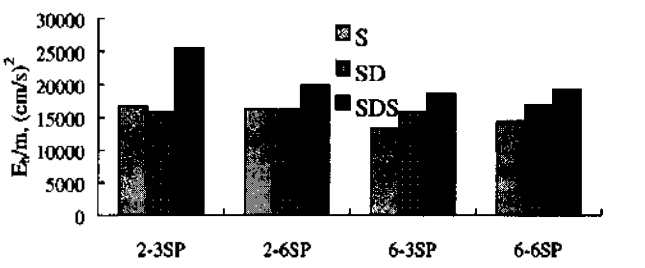

Fig. 11 Eh/m with EQ 5, DEQL II

Therefore, the authors conclude that the E_h is not always decreased but it can increase due to the increase of both

strength and stiffness. The E_h of frame SDS compared to frame S was not only smaller at lower intensity but also greater at higher intensity. Therefore, it is considered that the E_h is decreased when the intensity level is low, on the other hand, the E_h is dramatically increased with both the stiffness increase and period change. Thus, the increases of stiffness and strength of a frame can be contributed from the intensity of ground motion and the period change.

3.2 Strength Increase with the Same Stiffness (SD versus SDS)

From the pushover analysis, the stiffness of the frame 6SDS3 and 6SD3 were the same and the frame SDS had shorter period than that of frame SD (Fig. 6). The frame 6SDS6 and 6SD6 had the same situation. The effects of strength increase with the same stiffness on E_h were investigated based on the pushover analysis for 6-story frames (Fig. 8 to Fig. 11).

At the intensity level of DEQL I, the E_h of the SDS frames was smaller than that of SD frames except 2-3SP during EQ 1 and 5 (Fig. 8 to 9). The E_h of frame 6SDS was smaller than that of SD frames at DEQL I. It is believed that the reason of less E_h of frame SDS than that of frame SD is from the contribution of higher base shear coefficient (V/W). The seismic performance was increased by the increase of ductility in a system.

On the other hand, the E_h of frames was changed when the intensity of ground motion was increased from DEQL I to DEQL II. At EQ 1 with DEQL II, the E_h of 2-3SP and 2-6SP was increased with an increase of strength without any change of initial stiffness. At EQ 5 with DEQL II, the E_h of the frames was increased with an increase of strength without any change of initial stiffness. The E_h decreased with the increase of strength at both DEQL I and II (Fig. 9 and 10). Thus, the E_h with higher strength at the same stiffness condition was smaller than that of lower strength except EQ 5, DEQL II in this study. It is believed that the less E_h is contributed from the increased strength (V/W) of a global system.

3.3 Effect of Different Design Philosophies (SDS and MSD)

In this section, the E_h differences between the strength and drift control design (SD) and the strong-column and weak beam design (SDS) were investigated. The frame SD was modified to MSD to have the same structural properties in terms of structural period (T) and base shear coefficient (V/W). The 6MSD3 and 6MSD6 frames were modified from the frames of 6SD3 and 6SD6 respectively to match the period and base shear coefficient (V/W) to 6SDS3 and 6SDS6 frames. The natural period and V/W were the same as the ones of the 6SDS frames and the differences of the two were the plastic mechanism. The plastic hinges of frame MSD were mainly observed at columns. The plastic hinges of SDS frames occurred at the beams and columns.

At DEQL I, all frames were not sensitive to the total E_I and the total E_h to the five earthquakes. The differences on E_I and E_h between two systems were about 5% that was not significant for the nonlinear time history analysis. For the example of EQ 1, E_I/m was 2754 $(cm/s)^2$ for the 6SDS6 frames and 2812$(cm/s)^2$ for the 6MSD6 frame. The E_h/m was 54.32 $(cm/s)^2$ for the frame 6SDS6 and 54.77 $(cm/s)^2$ for the frame 6MSD6 under EQ 1 (Fig. 12). These patterns were also appeared in the other ground motions. The average differences in E_I/m and E_h/m were small by 3.1% and 5%, respectively. At EQ 5, DEQL I, the E_h was the same between the two systems as shown in Fig. 13. There were negligible differences for 6-3SP and 6-6SP during EQ 5, DEQL I.

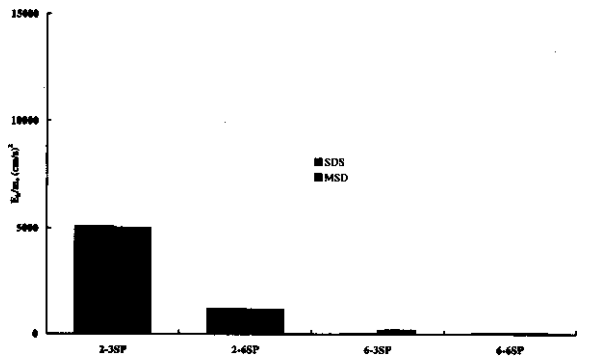

Fig. 12 E_h/m of SDS vs. MSD, EQ 1, DEQL I

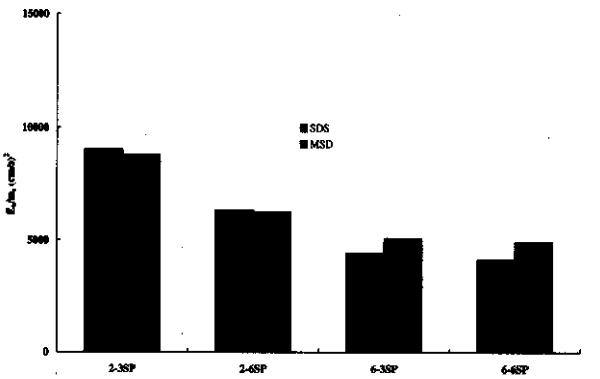

Fig. 13. Eh/m of SDS and MSD, EQ 5, DEQL II

At DEQL II, most of the frames showed small difference in E_h. The differences between 6SDS and 6MSD frames on E_h ranged from 0.1% to 24%, which means the difference of E_h for two frames is negligible with the increase of the intensity from DEQL I to DEQL II (Fig. 14 and Fig. 15). In the cases of EQ 4 and EQ 5, there were no significant differences on the energy demand between

two plastic mechanisms where the differences were ranged from 0.2 to 2.7%.

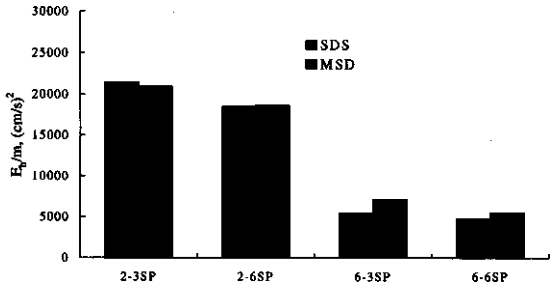

Fig. 14 Eh/m of SDS and MSD, EQ 1, DEQL II

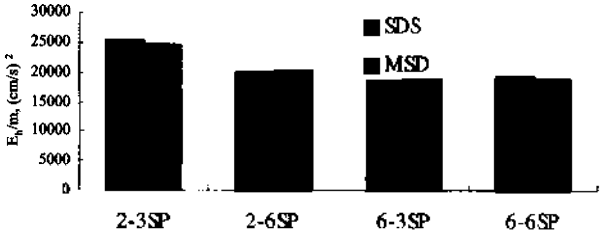

Fig. 15 Eh/m of SDS vs MSD, EQ 5, DEQL II

There was negligible E_h in beams because 6MSD6 frame was designed for the strength and drift (strong-beam and weak-column). Therefore, the E_h of columns was bigger than that of beam. In the observation of the E_h distribution over the floors, the damage of frame MSD concentrated on a weak member. Thus, frame SDS is much beneficial for seismic design to avoid the damage concentration at specific spot of members.

Conclusively, the E_h differences among various design philosophies were quite small. In the cases of EQ 1, 2 and 3, there were some differences ranging from 0.1 to 24% for both E_I and E_h that may be negligible. In this observation, the E_h difference around 20% is assumed negligible. In case of negligible difference of E_h for SDS and MSD frames, one can see some advantage of 6SDS6 from the E_h distribution over the floor. The E_h distribution over the floor of 6MSD6 frame, especially at the lower and upper floor, was increased to have more plastic deformation. The 6SDS frame showed better performance than the 6MSD frame in sharing the structural resistance to external forces.

3.4 Energy Expectation of Steel Moment-Resisting Frames

The mean E_h of MDOF systems are summarized in Fig. 16 and 17. The five earthquakes were summed and averaged to get the E_I and E_h in mean energy. The energy demands for the SDOF systems were quoted from the previous paper (Choi (1998) to compare with the results of MDOF system using the five ground motions. The second order of polynomial plot was used for the approximation of mean E_h for both SDOF and MDOF systems. In the E_h observation of SDOF systems, the base shear coefficient, η was used to explore the variation of yielding base shear, V_y. The base shear coefficient is the ratio of design base shear, V, to the yielding base shear, V_y. The base shear coefficient decreases with an increase of the yielding base shear coefficient. In this observation, the two base shear coefficients of 0.1 and 0.4 were used because the two values were comparable to the strength of the MDOF systems.

Because the E_h from MDOF systems generally differs from the one of SDOF systems, the E_h from SDOF system can be used with proper modification factor. The plots of SDOF systems were employed to grasp the range of disperse of the MDOF system to the SDOF system in terms of mean E_h. The variations of the mean E_h under DEQL I and II are shown in Fig. 16 and 17. Fig. 16 and 17 show two important meanings. First, the E_h of both systems decreases with the increase of the periods. In other word, the E_h of both systems increases with the increase of base shear coefficient (V/W). However, the E_h of short period systems for SDOF systems is sensitive. Second, the mean E_h of MDOF systems can be approximated from these figures. They explain the expectation of the mean E_h at the different design earthquake levels (DEQLs). The empirical equation could be drawn using the linear interpolation from the results;

$$E_h/m = \alpha\ (a) \times T + \beta\ (a), \quad 0.5 < T < 2.0 \qquad (1)$$

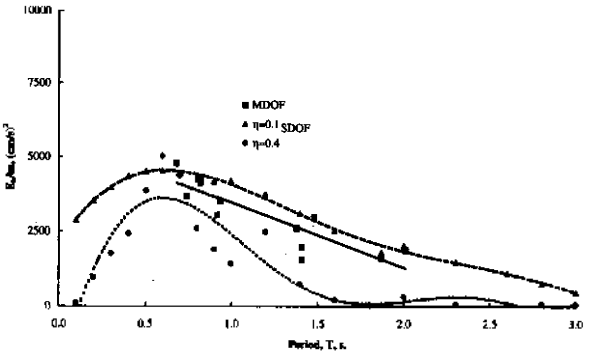

Fig. 16 Normalized mean hysteretic energy using 5 earthquakes, DEQL I

Since the results shows linear relationship between parameters such as mass, E_h, and T, a linear equation can be set up corresponding to E_h/m and T.

The function α (a) can be obtained from the curve of DEQL I and its equation can be expressed as $\alpha\ (a) = \alpha_0 a + \alpha_1$. The function β (a) can be obtained from another E_h dissipation curve at DEQL II and its equation can be expressed as $\beta\ (a) = \beta_0\ a + \beta_1$. The constant, a, is variable which can be expressed in terms of gravity acceleration. By the empirical calculation the following

constants are recommended; α_0 = -2957, α_1 = 550, β_0 = 9610, and β_1 = -2010.

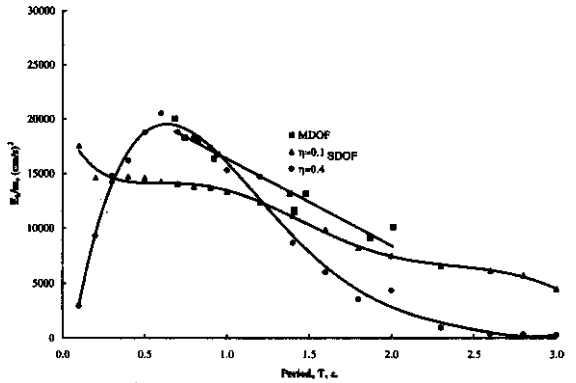

Fig. 17 Normalized mean hysteretic energy using 5 earthquakes, DEQL II

These constants are calculated by a = 0.3 and 0.6 where they represent DEQL I and DEQL II, respectively. In other word, they represent the peak ground acceleration of 0.3g and 0.6g. The negative signs represent the negative slope that the mean E_h dissipation is decreasing with the increase of the periods (Fig. 16 and 17). Since the periods of the examined MDOF systems are between 0.5 sec and 2.0 sec, the general equation is valid only in the limited regions. The formula can be used for the rough expectation of steel moment-resisting frames within the earthquake intensity levels, DEQL I and DEQL II. The total E_h dissipation of MDOF systems increased with the decrease of the period of the structures.

4. CONCLUSION

Various tasks were carried out to examine the energy characteristics for the steel moment-resisting frames and the following results could be drawn. The E_h dissipation decreased with an increase of stiffness and strength for lower and longer period structures with the peak ground acceleration (PGA) of 0.3g. However, this was not always true for the medium period regions under the PGA of 0.6g in both SDOF and MDOF systems. The E_h of MDOF systems increased when the stiffness and strength were increased at the increase of the PGA. The increase rate was ranged between 22% and 52% in case of Northridge Earthquake (EQ 5) with the PGA, 0.6g.

In the investigation of the effects of strength increase with the same stiffness, the E_h of strong column-weak beam control structure showed smaller E_h than the one of drift control structure at 0.3g. However, the result was reversed when the intensity level of ground motion was increased from 0.3g to 0.6g except the Northridge earthquake. Thus, the strength increase has an effect to increase the E_h during the increased earthquake ground motions. In the E_h observation of the drift control structure and strong column-weak beam control structure, the E_h between two design philosophies were negligibly small. The maximum difference in the six story three span structure model was 24%. The expectation of the mean E_h can be obtained from the suggested equation or by using the plot of the steel moment resisting.

This research, however, has following limitations. In the observation of the modified system, even though structural period and the yield shear force were the same, the structural mass was changed. In this research, only 5 earthquake ground motions were applied to get the empirical equation that was the function of mass and period. Thus, further investigations for the use of the proposed equation are necessary.

REFERENCES

Akiyama, H. (1985) *Earthquake-resistant limit state design. for buildings*. University of Tokyo Press

Arias, A. (1969) *A measure of earthquake intensity, MIT Press*, (pp. 438-469), Cambridge, England.

Banon, H., Biggs, J. M., & Irvine, H. M. (1981) Seismic damage in reinforced concrete frames, J. *of the Structural Division, ASCE*, 107(9), 1713-1729.

Berg, G. V. & Thomaides, S. S. (1960, July) Energy consumption by structures in strong-motion earthquakes, *Proceedings of the Second World Conference on Earthquake Engineering*, (pp. 11-18), Tokyo and Kyoto, Japan.

Choi, B. J. (1998, Dec.) *Performance-based seismic design of steel moment-resisting frames using energy approach*, Ph.D. Thesis, Illinois Institute of Technology, Chicago, IL.

Choi, B. J. (2000) An establishment of performance level threshold and design implementation using energy approach. *J. of the Archectural Institute of Korea. Structure & Construction*. 16(5), *in press*.

Fajfar, P. & Fischinger M. (1990) A seismic design procedure including energy concept, *Proceedings of the Ninth European Conference on Earthquake*, (pp. 312-321), Moscow.

Housner, G. W. (1956, June) Limit design of structure to resist earthquakes, *Proceedings of the World Conference on Earthquake Engineering*, Berkeley, CA.

Iwan, W. D. & Gates, N. C. (1979, May-June) The effective period and damping of a class of hysteretic structures, *Earthquake Engineering and Structural Dynamics*, 7(3), 199-211.

Kuwamura, H. & Galambos, T. V. (1989, June) Earthquake load for structural reliability, J. *of Structural Engineering*, 115(6).

Leger, P. and Dussault, S. (1992) Seismic-energy dissipation in MDOF structures, *J. of Structural Engineering*, 118(5), 1251-1269.

Load Resistant Factor Design (1995) AISI 1, Second Edition.

Nigam, N. C., & Jennings, P. C. (1968, June) *SPECEQ/UQ-digital calculation of response spectra from strong motion earthquake records*, California Institute of Technology, California.

Powell G. H, Parkash, V. & Campbell, S. (1993) *DRAIN-2DX BASE PROGRAM USER GUIDE*, U.C. Berkeley, CA.

Schneider, S. P., Roeder, C. W. & Carpenter, J. E. (1993, June), Seismic behavior of moment-resisting steel frames: experimental study, *J. of Structural Engineering*, 119(6).

Uang, C-M. & Bertero, V. V. (1990) Evaluation of seismic energy in structures. *Earthquake Engineering and Structural Dynamics*, 19, 77-90.

UBC-1997 (1997) *Uniform Building Code.*

Vidic, T., Fajfar, P. & Fischinger, M. (1991) On the hysteretic to energy ratio, *Proceeding of 6th Canadian Conference, Earthquake Engineering,* (pp. 69-76), Toronto.

Zarah, T., & Hall, W. J. (1984, Aug) Earthquake energy absorption in SDOF structures, *J. of Structural Engineering*, 110(8).

Notations

ξ	Viscous Damping
E_D	Damping Energy
E_I	Energy Input
E_h	Hysteretic Energy Input
E_k	Kinetic Energy
S_{pa}	Pseudo-acceleration
S_{pv}	Pseudo-velocity
t_D	Strong Ground Motion Duration
T	Fundamental Period
T_g	Predominant Ground Motion Period